Rev. Adv. Mater. Sci. 28 (2011) 200-206

INTERFACE ACTIVATED SINTERING OF TUNGSTEN BY NANO-PARTICLES IN THE SPARK PLASMA SINTERING

Joo Hyesook[1], Han Chulwoong[2], Kim Byungmoon[3], Kim Dohyang[1] and Choi Hanshin[2]

[1]Department of Advanced Materials Eng, Yonsei University, Seoul 120-749, South Korea
[2]Korea institute of industrial technology, Incheon 406-840, South Korea
[3]Division of energy and environment system, Dongguk University, Gyeongju 780-714, South Korea

Received: February 17, 2011

Abstract. Lots of engineering components have been produced by the powder metallurgy, especially for high melting point materials such as refractory metals and ceramics. Reduction in sintering temperature and/or sintering time results in reduced energy consumption and improved material properties in the powder metallurgy. Tungsten is a refractory metal and it is hard to obtain a full density sintered body. Main objective of this study is to make a high density tungsten sintered body at the reduced sintering temperature. Sintering is an interfacial phenomenon between contacting particles and it is a thermally activated process. In this regard, interface activations by both process and metallurgical aspects were considered. In the former process aspects, pulsed current directly passing through conductive particle surface makes Joule heating, micro-arcing, and electro-migration which are advantageous for enhancing mass flow during sintering. In the latter, it is well-known that the sintering temperature of nano-particles can be markedly reduced by the size effect. Tungsten nano-particles were synthesized by the pulse wire explosion process and then they were blended with micro-sized tungsten particles. In such a case, it could be proved that nano-particles existing at the interfaces between micro-particles played a homogeneous sintering activator when compared with other conventional irregular micro-particles and spheroidized micro-particles.

1. INTRODUCTION

Researches on the powder metallurgy have been extensively conducted and correspondingly industrial applications of powder metallurgy have been markedly enlarged [1]. As the powder metallurgy has become the crucial manufacturing technology for semi-final materials and final engineering components, both energy and material efficiencies need to be further improved in the coming climate change economics. In this regard, reductions in sintering temperature and/or sintering time are critical challenges in the green powder metallurgy. Tungsten is hard to be fully sintered because of its high melting point. In the conventional sintering process, it should be heated far above 2000 °C. In this case, energy loss is dramatically increased as the radiation heat transfer is dominant. According to the Stefan-Boltzman law of the radiation heat transfer, the radiation heat emission of a black body is proportional to the four power of a given temperature. When it comes to the emission of global warming gas such as carbon dioxide, it has a linear relationship with electrical energy consumption although the emission factor of electricity is quite different from countries. As a consequence, reduction of sintering temperature improves overall energy efficiency and also decreases emission of global warming gas. On the other hand, grain growth is also a thermally activated process during full density sintering. In gen-

Corresponding author: Choi Hanshin, e-mail: hschoi@kitech.re.kr

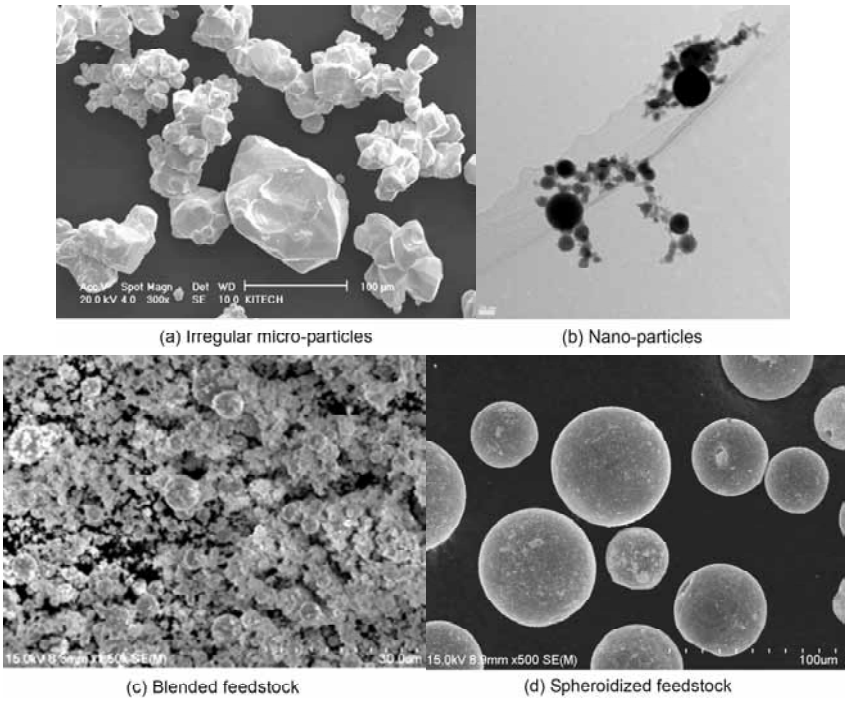

Fig. 1. Morphology of each feedstock.

eral, material properties of a fully sintered body are offset by density and grain size in the conventional sintering process. This is another motive for reducing sintering temperature. In order to make a full density tungsten body at the reduced sintering temperature, interface activations by both process and metallurgical aspects were considered in this study. Until now, advanced sintering processes such as induction sintering [2], micro-wave sintering [3], and electrical discharge sintering [4] have been developed. Among them, electrical discharge sintering is a well-established sintering process for engineering materials. Due to the pulse current, relatively high density can be achieved with the reduction in sintering time. In addition, it is proved that sintering temperature of nano-particle is drastically reduced by the extraordinary high surface to volume ratio but rapid grain growth and cost are still drawbacks in the industrial applications of nano-particles. Sintering is an interfacial phenomenon and the sintering kinetics is largely dependent on the particle size. Therefore, tungsten nano-particles were synthesized and then blended with micro-particles and the effects of the nano-particle addition on the sintering behavior were evaluated in view of the homogeneous sintering activator.

2. EXPERIMENTAL PROCEDURES

2.1. Feedstock material preparation

Three different kinds of tungsten feedstock particles were used in this study and the morphology of each particle can be seen in Fig. 1. Commercial tungsten micro-particles were bulky and irregular and the mean equivalent diameter was 70 um. Tungsten nano-particles shown in Fig. 1b were synthesized by the pulse wire explosion method in gas medium which is one of vapor phase condensation processes. Tungsten wire of 150 um was used at the applied voltage of 220 V. Median particle size was 12.7 nm and D_{90} was 23.8 nm by the TEM analysis and image analysis. Blended feedstock particles

Table 1. Summary of experiments.

Process	Feedstock	Peak temp. [°C]	Holding time [min.]	Heating rate [°C •min^{-1}]	Pressure [MPa]
Hot press	Irregular			20	
SPS	Irregular	1250, 1350, 1450, 1550	5	50	50
	Blended				

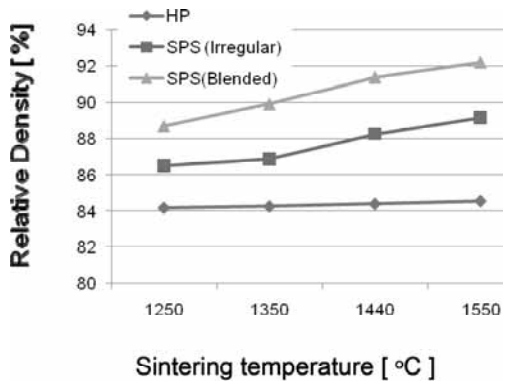

Fig. 2. Relative density variations according to sintering temperature.

were prepared by wet blending process using the nano-particles and the irregular micro-particles. Weight ratio of the micro-particles to the nano-particles was set to be 15. According to the blending time, particles were dried and the microstructures were examined after cold compaction. In view of the uniformity of the mixture, optimum blending time was 2 hours. Morphology of the blended feedstock is shown in Fig. 1c. By and large, nano-particles were agglomerated but well-dispersed with micro-particles. Finally, spherical micro-particles were prepared by the RF thermal plasma spheroidization. When irregular micro-particles were fed into the thermal plasma torch, they individually reacted with hot gas dynamics during flight. Heat and momentum transfer reactions make solid-state particle melt at the heating stage and then molten liquid particles are rapidly solidified at the subsequent cooling stage. During solidification, in-flight liquid particles are spheroidized to reduce their surface energy. Resulting particle morphology can be seen in Fig. 1d.

2.2. Sintering and characterization

To investigate the effects of the feedstock and the process on the sintering behaviors of tungsten, feedstock particles were sintered by both hot pressing process and spark plasma sintering process. Experimental parameters are summarized in Table 1. Graphite mold of which inner diameter was 15 mm was used for both processes and peak applied normal pressure was 50 MPa for all the experiments. In the case of thermal cycles, peak sintering temperature and holding time at the peak temperature were same regardless of sintering process. However, heating rate for the hot pressing process was 20 °C·min^{-1} while particles were heated at the heating rate of 50 °C·min^{-1} in the spark plasma sintering. After sintering, surface was sufficiently removed to exclude possible interaction between tungsten and graphite. Absolute density of the sintered body was

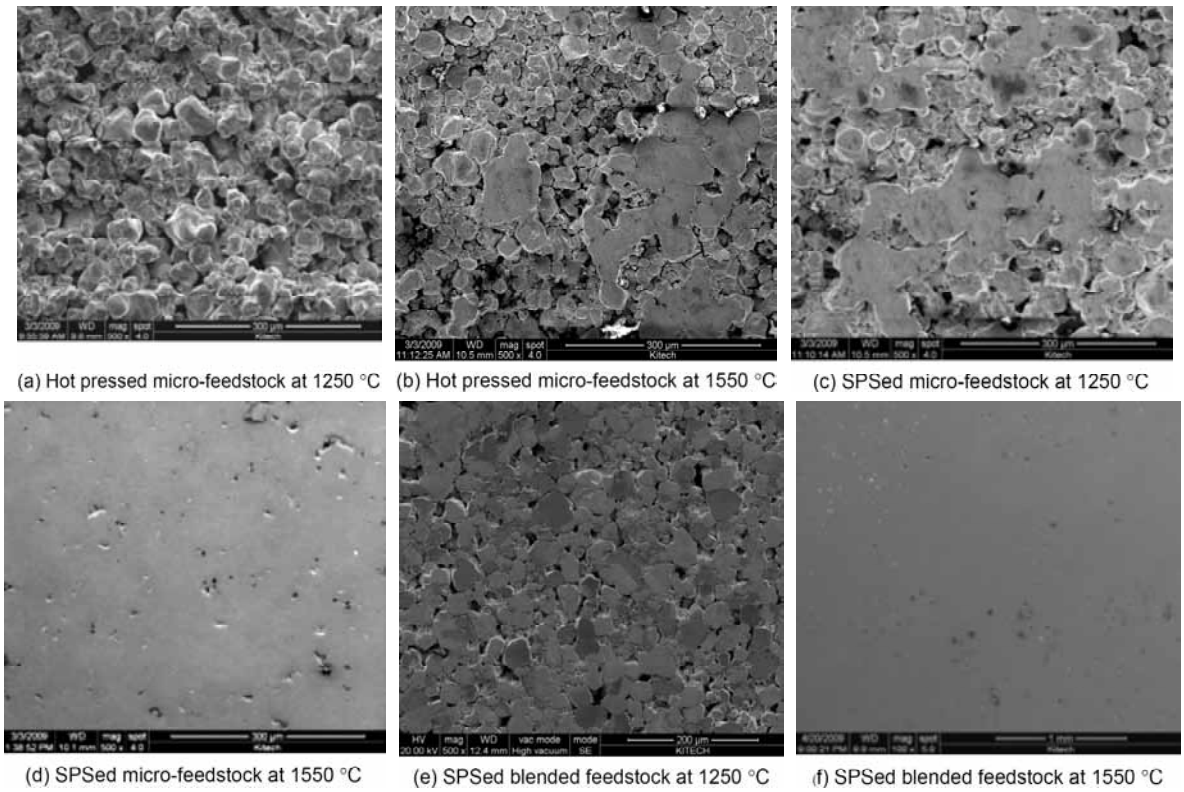

Fig. 3. Representative microstructures of sintered bodies.

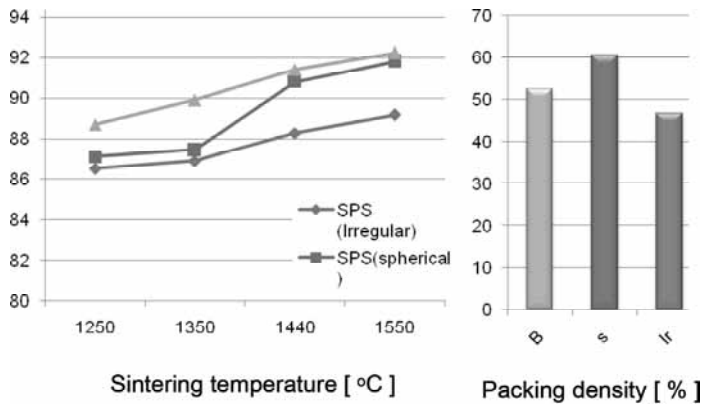

Fig. 4. Packing density effects on the relative density.

measured by the Archimedean method and relative density was calculated by dividing it with the theoretical density of tungsten. Micro-structure of as-sintered body was examined using a scanning electron microscope and also electron backscattered diffraction was conducted for the sintered bodies made of blended feedstock in order to verify the microstructure evolution.

3. RESULTS AND DISCUSSION

Effects of the process and the addition of nano-particles on the relative density of the sintered tungsten can be seen in Fig. 2 and the representative microstructures of the as-sintered tungsten bodies are shown in Fig. 3. In the case of the process effects, irregular micro-particles were sintered by the hot pressing process and the spark plasma sintering process. At the all the sintering temperatures, relative density of tungsten by the spark plasma sintering is higher than by the hot pressing process even though overall sintering time is much shorter. Within the scope of the sintering temperature, further densification is observed in the spark plasma sintering as the sintering temperature is increased. However, there is little difference of relative density in the hot pressing process. For the hot pressed tungsten at 1250 °C of Fig. 3a, it shows a typical morphology at the initial sintering stage. As the sintering temperature is increased to 1550 °C , significant neck growth and local densification are observed as shown in Fig. 3b. Meanwhile, microstructure of the spark plasma sintered tungsten at 1250 °C (Fig. 3c) is similar with that of the hot pressed one at 1550 °C. For the SPSed at 1550 °C of Fig. 3d, dense microstructure with closed pores is observed. Correspondingly, it could be confirmed that the spark plasma sintering is much effective to make a full-dense sintered body than the conventional hot pressing at the same thermo-mechanical cycle. As far as the feedstock effects are concerned, sintered bodies made of blended feedstock are much denser than micro-particles at all the sintering temperatures in the spark plasma sintering. Further densification for the blended feedstock could be observed with the increase of sintering temperature and the relative density is as much as 92% at the peak sintering temperature of 1550 °C. It is also confirmed from the microstructures of Figs. 3e and 3f. Through the results, it is empirically verified that interface can be effectively activated by the spark plasma sintering and the addition of nano-particles.

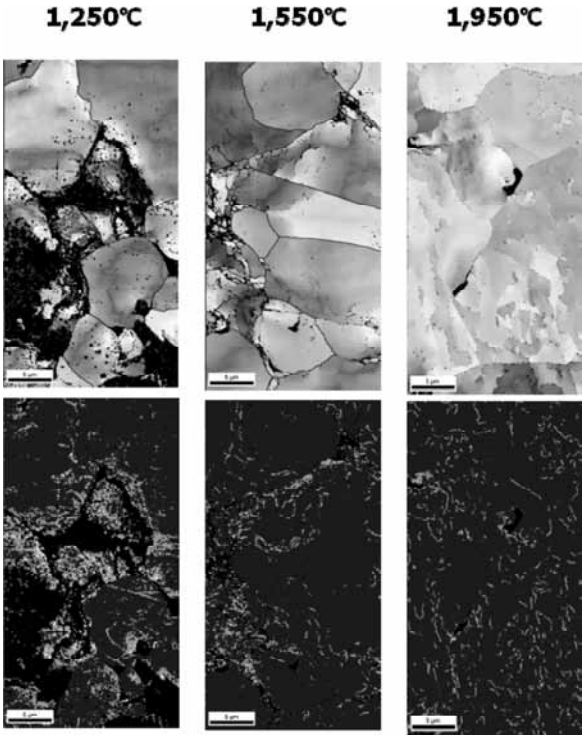

Fig. 5. EBSD analysis of spark plasma sintered W bodies using blended feedstock (a:Image quality(IQ) map, b: Kernal average Misorientation(KAM)map).

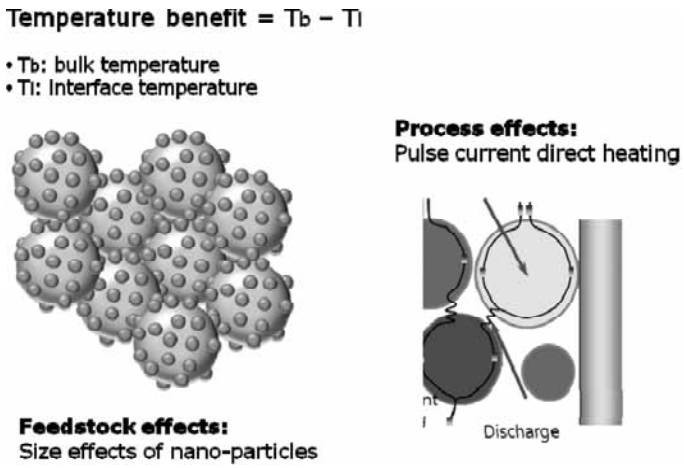

Fig. 6. Possibility of temperature benefit resulted from nano-particle addition and pulse current.

According to the microstructural evolution and sintering mechanism, sintering is divided into three stages: initial stage, intermediate stage, and final stage. In the initial stage, formation and growth of sinter neck occur. As the particle size is reduced, sintering stress by the curvature is increased. Therefore, mass transport to sinter neck is enhanced with the reduction of particle size. Moreover, it is known that the surface diffusion and grain boundary diffusion are dominant for the fine particles [1]. As a result, the addition of nano-particles enhances sintering ability even at the reduced sintering temperature. Apart from the particle size, packing density also has an influence on the initial stage of sintering. With packing density increasing, sintering kinetics at the initial stage is known to be increased. To verify whether the enhanced sintering kinetics by the addition of nano-particles comes from the packing density effects, spheroidized micro-particles were also sintered by the spark plasma sintering process. Relative density variation of spherodized feedstock is compared with that of other feedstock and the packing density of each feedstock is also shown in Fig. 4. Packing density of irregular feedstock, spherical feedstock, and blended feedstock was 46.6%, 52.6%, and 60.5%, respectively. Packing density of spheroidized feedstock is the highest among the feedstock. Denser sintered body can be obtained by replacing irregular micro-particles with spherical ones. However, blended feedstock still shows higher density than the spherical particles at the all the sintering temperature. It is worthwhile to note that the effects of the addition of nano-particles on density are dominant in relative low temperature when compared with the spherical micro-particles: above 1450 °C, relative density and variation of blended feedstock shows similar with those of spherical feedstock. Accordingly, it can be deduced that nano-particles have dominant roles in sintering at low temperature but activation power of nano-particles is diminished as sintering proceeds.

Fig. 5 shows the EBSD results of the SPSed tungsten which were sintered at 1250 °C, 1550 °C, and 1950 °C using the blended feedstock: (a) is image quality map and (b) is Kernal average misorientation map. For the sintered body at 1250 °C, significant amount of fine grains are still observed mainly around the particle boundaries. As the sintering temperature is increased, grain growth is notable. However, grain growth around the particle boundaries is prominent at 1550 °C while grain growth within the micro-particle seems to be negligible. At the further increased temperature at 1950 °C, the relative density reached 97% and it is hard to find sub-micron grain in the sintered body. In accordance with microstructures, stress distribution is also estimated by the Kernal average misorientation map. As the sintering temperature is increased, stress intensity at the particle boundary is markedly diminished. It is equivalent with relative density variation of the blended feedstock. Addition of nano-particles played a critical role in sintering at the low temperature and resulting sintering kinetics was accelerated. However, coagulation of nano-particles means the reduction of the activation power of nano-particles.

Particles are sintered together via mass flow to reduce surface energy when a sufficient energy is provided. Therefore, enhanced mass transport by increasing driving force or kinetics can effectively reduce the sintering temperature and this is referred to as the activated sintering. In order to reduce the

sintering temperature in full-density tungsten sintering, interface activations were considered in this study. Basic concept for the suggested interface activation is schematically represented in Fig. 6. Temperature benefit between a virtual interface temperature and a bulk temperature (process temperature) can be an estimate for the interface activation degree. It can be assumed that enhancement of mass flow during sintering has an effect on the increase of interface temperature at the constant process temperature. In the case of feedstock effects, the addition of nano-particles on the micro-particles results in the virtual interface temperature. As shown in Fig. 2, relative density of sintered body using nano-particle and micro-particle blended feedstock is about 89% at the sintering temperature of 1250 °C. However, sintering temperature needs to be higher than 1450 °C in the case of irregular micro-particles. Therefore, temperature benefit is at least 200 °C in this case. In the case of tungsten, chemical additives such as Pd, Ni, Fe, and Cu are intentionally added to reduce the sintering temperature. In such a case, tungsten is dissolved into the chemical additive phase which surrounding tungsten particle. Thus, the tungsten diffusion path and kinetics with the additive is quite different from pure tungsten. Similar with the heterogeneous chemical additive, a homogeneous sintering activator which can enhance sinterability was considered and the feasibility of tungsten nano-particle as a homogeneous sintering activator was evaluated. It is well-known that the sintering temperature of nano-particles is far lower than that of micro-particles. As a matter of fact, a homologous sintering temperature which is the absolute sintering temperature divided by the absolute melting temperature is largely dependent on the particle size. In the case tungsten, homologous sintering temperature is markedly reduced to $0.2T_m$ to $0.4T_m$ for nano-particles while it is $0.5T_m$ to $0.8T_m$ for micro-particles. [5] Higher surface energy of nano-particles results in the increase of the driving force for sintering. Also, sintering stress and stress gradient of contacting particles accelerate mass flow because the sintering stress between particles is inversely proportional with the particle size [8]. Moreover, material transports such as surface diffusion, grain boundary diffusion, mechanical rotation, and viscous flow are enhanced in nano-particles [6,7]. Therefore, sintering between nano-particles and between nano-particle and micro-particle can occur at the relatively low process temperature by the size effects. This is regarded as a kind of interface activation by the feedstock tailoring. On the other hand, Joule heating on the particle surface, possible micro-arcing between particle surfaces, and enhancement of electro-migration of diffusing species result from the pulse current directly passing through the conductive particles [9-11]. Therefore, virtual interface temperature is considered to be higher than bulk temperature: heat is directly generated around the particle surface in the spark plasma sintering. Surface cleaning effects by the possible micro-arcing between particle surfaces may reduce the activation energy for neck formation by removing surface oxide layer. According to the literature [12], electric filed results in the mass flow and the electro-migration can be considered to enhance kinetics of sintering. Accordingly, pulse current effectively increases the virtual interface temperature when compared with the conventional hot pressing process. Through the results, it is empirically proved that the addition of nano-particles and selection of pulse current can increase temperature benefit in sintering.

4. CONCLUSION

Effects of sintering process and feedstock on the sintering behaviors of tungsten were investigated in this study and it could be empirically proved that current discharge heating in the spark plasma sintering and also the addition of nano-particles are advantageous for reducing sintering temperature. Pulse current passing through the conductive particles results in the increase of virtual interface temperature at a certain process temperature when compared with the conventional hot pressing process in that Joule heating around the particle surface, cleaning of particle surface by micro-arcing, and enhancement of diffusion by electric field are expected. On the other hand, tungsten nano-particles were intentionally added to act as homogeneous sintering activator in this study in order to reduce sintering temperature for refractory tungsten micro-particles. Tungsten nano-particles existing on the tungsten micro-particles are effective for activating sintering at low temperature owing to the size effects. It can be deduced that the sintering stress between nano-particles and also nano-particle and micro-particle makes mass transport enhanced in the case of nano-particle addition. With the sintering temperature increasing, higher density was achieved as the sacrifice of the driving force of nano-particles. Conclusively, it could be empirically proved that the sintering temperature of tungsten micro-feedstock can be much lowered by blended feedstock in the spark plasma sintering.

REFERENCES

[1] R.M. German, *Powder metallurgy and particulate materials processing* (Metal powder industries federation, 2005).
[2] M. Dewidar // *Materials and design* **31** (2010) 3964.
[3] A. Mondal, A. Upadhyaya and D. Agrawal // *Int. Jr of Ref. Met. and Hard Mat.* **28** (2010) 597.
[4] R. Orru, R. Licheri, A.M. Locci, A. Cincotti and G. Cao // *Materials science and engineering R* **63** (2009) 127.
[5] J.R. Groza // *Int J Powder Metall* **35** (1999) 59.
[6] X. S. Arcidiacono, N.R. Bieri, D. Poulikakos and C.P. Grigoropoulos // *Int. Jr. of Multiphase Flow* **30** (2004) 979.
[7] Y. P. Zeng, S. Zajac, P.C. Clapp and J.A. Rifkin // *Materials science and engineering A*.**252** (1998) 301.
[8] R.M. German, *Sintering theory and practice* (John Wiley and sons, 1996).
[9] Z.A. Munir, U.A. Tamburini and M. Ohyanagi // *Jr. Mater. Sci.* **41** (2006) 763.
[10] Z. Shen, M. Johnsson, Z. Zhao and M. Nygren // *J. Amer. Ceram. Soc.* **85** (2002) 1921.
[11] E. Olevsky and L. Froyen // *Scripta materialia* **55** (2006) 1175.
[12] R.E. Hummel // *Int. Mater. Rev.* **39** (1994) 97.